Convergent evolution of cell size enables adaptation to the mangrove habitat

Guo-Feng Jiang[1, *] Bo-Tao Qin[1], Long-De Luo[1], Qi-Xia Li[1], Li-Ming Xu[2], Li Xu[3], Arezoo Dastpak[4], Kevin A. Simonin[5], Adam B. Roddy[6, *]

[1]Guangxi Key Laboratory of Forest Ecology and Conservation, Guangxi Colleges and Universities Key Laboratory for Cultivation and Utilization of Subtropical Forest Plantation, and State Key Laboratory for Conservation and Utilization of Subtropical Agro-Bioresources, College of Forestry, Guangxi University, Daxuedonglu 100, Nanning, Guangxi 530004, China;

[2]Industrial Technology Engineering Center for Zhuang & Yao Medicinal Organisms, Botanical Garden of Zhuang & Yao Medicinal Plants, Collaborative Innovation Center of Great Health, College of Medicine and Health Care, Guangxi Vocational & Technical Institute of Industry, Nanning, Guangxi 530001, China;

[3]Key Laboratory of Tropical Marine Ecosystem and Bioresource, Fourth Institute of Oceanography, Ministry of Natural Resources, Beihai, Guangxi 536000, China;

[4]Institute of Environment, Department of Biological Sciences, Florida International University, Miami FL 33199 USA;

[5]Department of Biology, San Francisco State University, San Francisco, CA 94132 USA;

[6]Department of Environmental Studies, New York University, New York, NY 10012 USA.

*** Correspondence:** Guo-Feng Jiang **(**gfjiang@gxu.edu.cn), Adam B. Roddy **(**adam.roddy@nyu.edu**)**

Lead Contact: Adam B. Roddy **(**adam.roddy@nyu.edu**)**

SUMMARY

Mangroves have evolved at least 27 times across ~20 plant families to survive coastal environments characterized by high salinity, inundation, intense light, and strong winds [1,2]. To survive these extreme conditions, mangroves exhibit a variety of physiological strategies to tolerate the low osmotic potentials associated with saltwater inundation [3-8]. Because low osmotic potentials are counterbalanced by high turgor pressure, saltwater exposure exerts mechanical demands on cells. Analyzing 34 mangrove species and 33 closely related inland taxa from 17 plant families, we show that compared to their inland relatives, mangroves have unusually small leaf epidermal pavement cells and thicker cell walls, which together confer greater mechanical strength and tolerance to low osmotic potentials. However, mangroves do not exhibit smaller, more numerous stomata that enable higher photosynthetic rates [9-11], suggesting selection on biomechanical integrity rather than on gas exchange capacity. Notably, mangroves break the allometric scaling between the sizes of epidermal pavement cells and stomata typically seen in land plants [3,12], highlighting that strong selection in saline habitats can override genome size–mediated scaling rules. Phylogenetic comparative analyses revealed repeated convergent evolution of cell traits across independent transitions from inland to coastal habitats. These anatomical changes constitute a simple but effective adaptation to salt stress. Our findings underscore the role of biomechanics in driving convergent evolution of cell traits and suggest that manipulating cell size and wall properties could be a promising strategy to engineering salt-tolerant plants.

RESULTS AND DISCUSSION

As the outermost layer of cells, the epidermis represents a direct physical connection between plants and their environment. In leaves, the epidermis regulates the exchange of CO_2 and water with the atmosphere [13], protects leaves from mechanical damage, and provides biomechanical strength [14,15]. The leaf epidermis is generally composed of four cell types (pavement cells, guard cells, subsidiary cells, and trichomes), each of which perform functions that are influenced by their cell size, cell shape, and cell packing density. For example, variation in the size, shape, and density of pavement cells, which constitute most of the epidermis, directly influence both leaf mechanical strength and the distribution of stomatal guard cells that regulate leaf gas exchange [12,14,16].

Because of their direct effects on leaf gas exchange and whole plant carbon gain, the size, shape, and density of leaf epidermal cell types often vary in predictable ways with environmental conditions [12,14]. For example, declines in stomatal size and increases in stomatal density occurred among early Cretaceous angiosperms allowing them to maintain high rates of CO_2 diffusion into the leaf despite declining atmospheric CO_2 concentrations [9-11]. These changes in cell size and cell packing density corresponded with changes in genome size due to a positive scaling between genome size and both minimum cell size and maximum cell packing density among all leaf cell types [9,17,18]. Over developmental timescales, leaf acclimation to light intensity and humidity depends on differential expansion of pavement cells, which regulates the spacing of stomata, independent of genome size [12,19]. Because developmental acclimation to the environment is an inherently biomechanical process, building leaves to maintain positive leaf carbon balance in environments differing in water availability depends on the biomechanical traits that influence cell and tissue expansion [20-22].

Though often overlooked, the biomechanical properties of cells and tissues are mechanistically linked to leaf water balance [12,20,23,24]. Maintaining water balance is particularly challenging for plants growing in saline environments. Salt-tolerance is one of the rarest adaptations among vascular plants. In particular, tropical plants that define the mangrove ecosystem consist of only ~70 species spanning ~20 lineages of vascular plants,

and the mangrove habit has evolved independently at least 27 times over the past 50 million years [1,2]. The high salinity, intense sunlight, and frequent wind exposure characteristic of the mangrove habitat have led to various physiological strategies to prevent desiccation, including salt exclusion, salt secretion, and extreme tolerance to the low osmotic potentials incumbent upon cells exposed to salt–all of which influence mangrove hydraulics and photosynthesis [3-8].

Epidermal pavement cells are particularly important for regulating leaf water balance in mangroves because they are the first cells impacted by salt spray and because epidermal pavement cells often regulate guard cell turgor pressure and stomatal conductance [25,26]. Because physiological function requires high water potentials, cells exposed to salt must counteract more negative osmotic potentials with high turgor pressure. Turgor pressure is generated by rigid cell walls that prevent cell expansion as water moves into the cell. Compared with freshwater and terrestrial plants, marine plants possess stiffer cell walls that generate higher turgor pressures under low osmotic potentials [27]. Because epidermal pavement cells begin development small in size and shaped as polyhedral and take on increasingly lobed shapes as they expand [21,28], cells with more negative osmotic potentials may not expand and change shape as much as cells with less negative osmotic potentials [29,30]. Furthermore, all else being equal, smaller cells are mechanically stronger than larger cells [31,32]. These relationships between osmotic potential, cell wall properties, cell size, and cell shape suggest that adaptation to the saline coastal environment may have resulted in convergent evolution of cell size, cell shape, and cell wall properties.

Here we tested whether cell size, cell shape, and cell wall thickness exhibit repeated, convergent evolution in association with adaptation to the mangrove habitat. We sampled 34 mangrove species (including 24 true mangroves and 10 mangrove associates) and 33 of their inland relatives (non-mangroves) from 17 plant families (Key Resources Table), representing at least 18 independent transitions between coastal and inland habitats and representing the majority of mangrove lineages. Given their shared ancestry, repeated directional divergence in these traits between mangroves and inland relatives would provide strong evidence for

convergent evolution of leaf anatomy. We predicted that mangroves would have smaller cells exhibiting less lobed cell shapes and thicker cell walls, even after accounting for allometric scaling of cell size among different cell types.

We sectioned and cleared leaves prior to microscopic imaging and manually measured anatomical traits (see Methods). We combined phylogenetic and non-phylogenetic analyses to characterize differences in traits and trait relationships between mangroves and non-mangroves. Using ANOVAs that accounted for phylogenetic relatedness (Figure 1), we found that compared to closely related non-mangroves mangroves had significantly smaller epidermal pavement cells (S_{ec}; $F = 14.64$, $P < 0.001$), a significantly lower ratio of epidermal cell size to stomatal size (S_{ec}:S_s; $F = 25.14$, $P < 0.001$), epidermal cells with significantly less lobed shapes ($\mathcal{A}$; $F = 15.94$, $P < 0.001$), and thicker cell walls of epidermal pavement cells (T_{ec}; $F = 8.40$, $P < 0.01$), palisade mesophyll cells (T_{pal}; $F = 8.44$, $P < 0.001$), and spongy mesophyll cells (T_{spo}; $F = 10.15$, $P < 0.001$). However, there was no significant difference between mangroves and non-mangroves in stomatal size (S_s; $F = 3.11$, $P = 0.05$), stomatal density (D_s; $F = 0.07$, $P = 0.78$), or modeled maximum stomatal conductance ($g_{s,max}$; $F = 0.38$, $P = 0.55$; Figure 1), suggesting that selection on cell size was not due to selection for smaller or more densely packed stomata that elevate photosynthetic capacity but instead specifically on epidermal pavement cell size and cell wall thickness.

Other periods of strong environmental selection, such as during early Cretaceous climate change, resulted in smaller cells enabled by smaller genomes among the angiosperms [9-11]. However, mangrove lineages include even ferns of the family Pteridaceae, which typically have large genomes, suggesting that adaptation to saline environments may not require genome size reductions. If selection has favored smaller cells in mangroves, then cell and genome sizes may scale differently among mangroves and non-mangroves. Indeed, for a given genome size mangroves exhibited significantly smaller epidermal pavement cells than non-mangroves (i.e. lower intercept; mangrove intercept = 2.40 [2.31, 2.48], non-mangrove intercept = 2.58 [2.39, 2.76]; $t = -4.25$, $df = 25$, $P < 0.001$; Figure 2A). Mangroves also exhibited a shallower slope than non-mangroves in the scaling of epidermal pavement cell

size with genome size (mangrove slope = 0.66 [0.51, 0.84], non-mangrove slope = 1.01 [0.70, 1.45]; r = -0.58, df = 25, P < 0.01; Figure 2A). Though cell sizes are typically coordinated among different cell types in a leaf [9], there was no coordination between epidermal pavement cell size and stomatal size among mangroves (P = 0.76) even though there was strong coordination among non-mangroves (R^2 = 0.64, P < 0.0001, Figure 2B). Thus, even after accounting for variation in genome size and stomatal size, mangroves have smaller epidermal cells than closely related inland plants.

To further test how traits evolved among mangrove and non-mangrove lineages, we compared Brownian motion and Ornstein-Uhlenbeck (OU) models of trait evolution using T_{ec}, S_{ec}:S_s, and $\mathcal{A}$, sampled across 1000 histories of habitat occupation modeled using stochastic character mapping [33]. The single-optimum OU model was the best fit across all 1000 histories of habitat occupation (Figure S2). However, for models using only T_{ec} and S_{ec}:S_s, the OU process with different optimum trait values for mangroves and non-mangroves was the best fitting model across all 1000 histories (Figure S3). In these models, mangroves were estimated to have thicker optimal T_{ec}, lower optimal S_{ec}:S_s, and lower optimal $\mathcal{A}$ (Figure 3). These results reiterate that mangrove lineages–including both ferns and angiosperms–have experienced selection primarily for smaller epidermal pavement cells and thicker cell walls.

Additionally, we tested for convergent evolution of anatomical traits among mangroves and non-mangroves using a method that lacks *a priori* designation of habitat affinity and instead finds unique selective regimes on the phylogeny [34] based solely on the phylogeny and trait data (Figure 3 and S4). Though not all of the mangroves we sampled were recovered as being in selective regimes distinct from their non-mangrove relatives, the most iconic true mangroves (Rhizophoraceae, Acanthaceae, Combretaceae, and Lythraceae) [2] were identified as being in the same selective regime and distinct from non-mangroves, indicative of convergent evolution of leaf anatomy.

Overall, these results point to two key adaptations to the saline coastal environment. First, thicker cell walls enable cells to withstand the greater turgor pressures needed to compensate

for the lower osmotic potentials associated with salt exposure [3,4,27]. Though cell wall microstructure and biochemistry influence cell wall mechanical properties [35], all else being equal, thicker cell walls should be mechanically stronger. Interestingly, palisade and spongy mesophyll cell walls were also thicker in mangroves (Figure 1 H and I), which could limit CO_2 diffusion into mesophyll cells [36-38], suggesting that meeting biomechanical demands may be so important to mangroves as to be worth any cost to photosynthesis.

Second, smaller epidermal pavement cells may further increase tolerance to low osmotic potentials. The reduction of epidermal pavement cell size relative to stomatal size suggests that selection in saline environments not only favors small epidermal cells *per se* but also favors breaking the typical coordination between epidermal and stomatal sizes (Figure 2B). Across vascular plants there is typically strong coordination in the sizes of cells across tissues with this allometric scaling being coordinated largely by genome size variation [9]. However, selection in saline coastal environments is evidently strong enough to overcome this usual coordination among cell sizes. Though reducing genome size has been one way of reducing minimum cell size, smaller epidermal cells have evolved among mangroves regardless of any changes in genome size (Figure 2A).

While smaller cells have been shown to be beneficial during periods of declining atmospheric CO_2 concentration[9,10], our results point to an additional benefit of smaller cells during adaptation to saline coastal environments. That smaller epidermal pavement cells have evolved repeatedly among mangrove lineages regardless of genome and stomatal sizes highlights the role of natural selection in shaping plant phenotypes. Furthermore, this repeated, convergent evolution as lineages have colonized the saline coastal environment suggests that cell size, cell shape, and cell wall thickness are highly labile traits that may be targets for engineering increased salt tolerance. These traits likely represent an integrated response to the simultaneous demands of maintaining mechanical integrity, regulating water loss, and sustaining photosynthesis in saline environments. These results also suggest that though more complex anatomical and physiological adaptations, such as salt secretion, may

be important adaptations for some mangroves, reducing cell size may be a relatively simpler modification that does not depend on evolving new cell types and tissue arrangements.

RESOURCE AVAILABILITY

Lead Contact: Adam B. Roddy (adam.roddy@nyu.edu)

Materials Availability

This study did not generate unique reagents.

Data and Code Availability

- Data: Trait data have been deposited at OSF.io and are publicly available as of the date of publication at **10.17605/OSF.IO/HD9T6**.

- Code: This paper does not report original code. Example code for plotting trait data on the phylogeny is publicly available at OSF.io as of the date of publication at **10.17605/OSF.IO/HD9T6**

- Additional Information: Any additional information required to reanalyze the data reported in this paper is available from the lead contact upon request.

SUPPLEMENTAL INFORMATION

Supplemental information can be found online.

ACKNOWLEDGMENTS

We thank the mangrove natural reserves and botanical gardens, for providing access to plants and help in field sampling. We gratefully thank the large scientific instrument sharing platform of State Key Laboratory for Conservation and Utilization of Subtropical Agro-Bioresources for providing technical support. This work was supported by grants from the National Natural Science Foundation of China (grant number 32460373), Guangxi Science and Technology Base and Talent Special Project (Guikesci AD25069066), the Natural Science Foundation of Guangxi Province (Key Program 2022GXNSFDA035059), a grant from Key Laboratory of Tropical Marine Ecosystem and Bioresource, Ministry of Natural Resources (grant number 2024ZD02), and the Bama county program for talents in science and technology, Guangxi, China (20220011) to G-FJ. It was also supported by Guangxi Technology Plan Project (Guikesci AD25069098). ABR was supported by US National Science Foundation grant numbers IOS-2243971, CMMI-2414269, and CMMI- 2532425.

AUTHOR CONTRIBUTIONS

A.B.R and G.-F.-J. conceptualized the project. G.-F.J. directed the research. B.-T.Q., G.-F.J., L.-D.L., Q.-X. L., L.-M.X., L.X., and A.D. collected the data. A.B. R., B.-T. Q., K.A.S., and G.-F.J. analyzed the data. G.-F.J. and A.B. R. wrote the manuscript, and all authors reviewed and revised each draft before giving approval for submission of the final version.

DECLARATION OF INTERESTS

The authors declare that they have no conflict of interest.

FIGURE LEGENDS

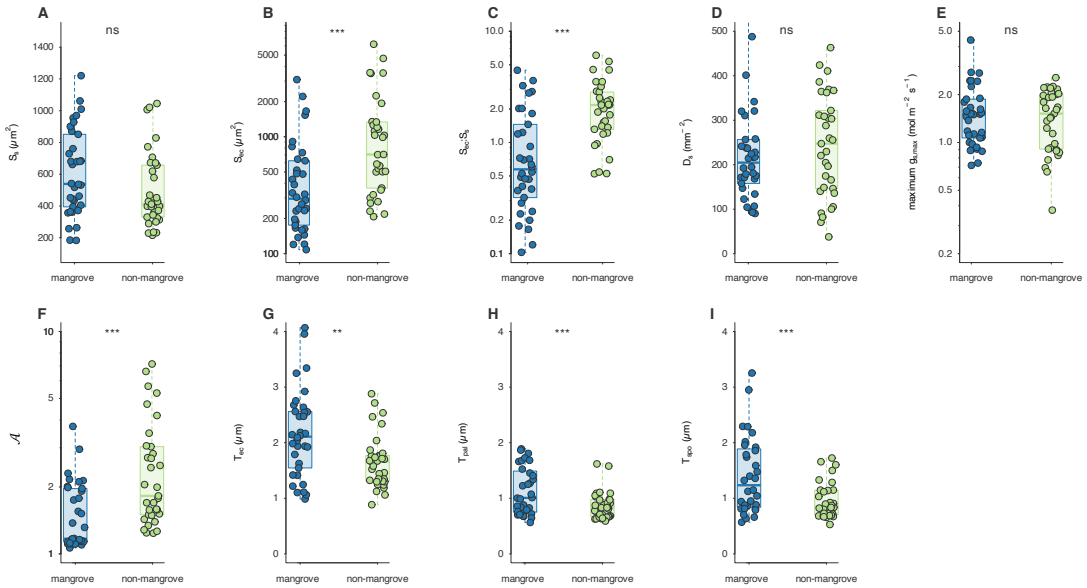

Figure 1. Trait differences between mangroves and non-mangroves. Mangroves and mangrove associates differ significantly from non-mangroves in anatomical traits related to cell biomechanics but not to traits related to gas exchange: compared to non-mangroves, mangroves exhibited (A) no difference in stomatal size ($F = 3.11$, $P = 0.05$), (B) smaller epidermal pavement cell size ($F = 14.64$, $P < 0.001$), (C) lower ratio of epidermal pavement cell size (S_{ec}) to stomatal size (S_s) ($F = 25.14$, $P < 0.001$), (D) no difference in stomatal density ($F = 0.07$, $P = 0.78$), (E) no difference in anatomical maximum stomatal conductance ($F = 0.38$, $P = 0.55$), (F) lower epidermal pavement cell shape acircularity ($F = 15.94$, $P < 0.001$), (G) thicker epidermal pavement cell walls ($F = 8.40$, $P < 0.01$), (H) thicker palisade cell walls ($F = 8.44$, $P < 0.001$), and (I) thicker spongy mesophyll cell walls ($F = 10.15$, $P < 0.001$). Points represent species mean trait values, and analyses are based on phylogenetic analysis of variance. **P < 0.01; ***P < 0.0001, ns = not significant

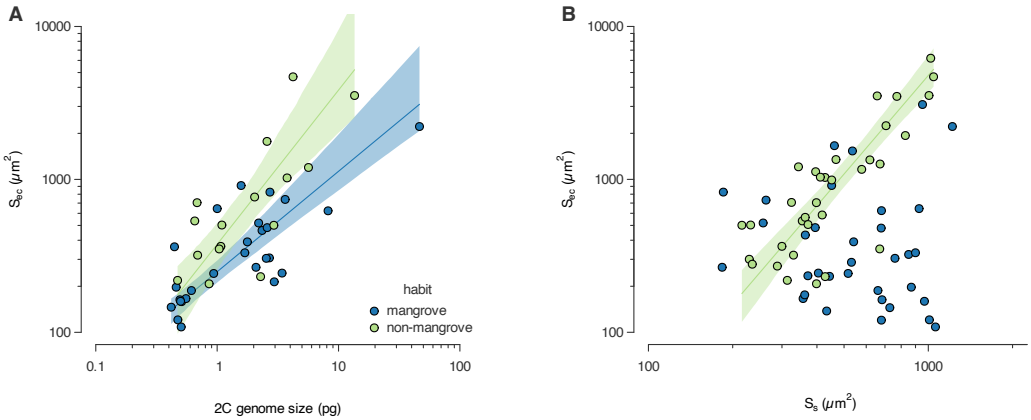

Figure 2. Mangroves deviate from the typical scaling of cell and genome sizes.

Mangroves differed from non-mangroves in the scaling of genome size, epidermal cell size, and stomatal size. (A) Genome size was a strong predictor of epidermal cell size for both mangroves ($R^2 = 0.62$, $P < 0.0001$) and non-mangroves ($R^2 = 0.57$, $P < 0.001$), though mangroves exhibited smaller epidermal cell sizes across all genome sizes than non-mangroves. (B) Stomatal size and epidermal pavement cell size were strongly coordinated among non-mangrove inland plants ($R^2 = 0.64$, $P < 0.0001$), but there was no relationship among mangroves ($P = 0.76$).

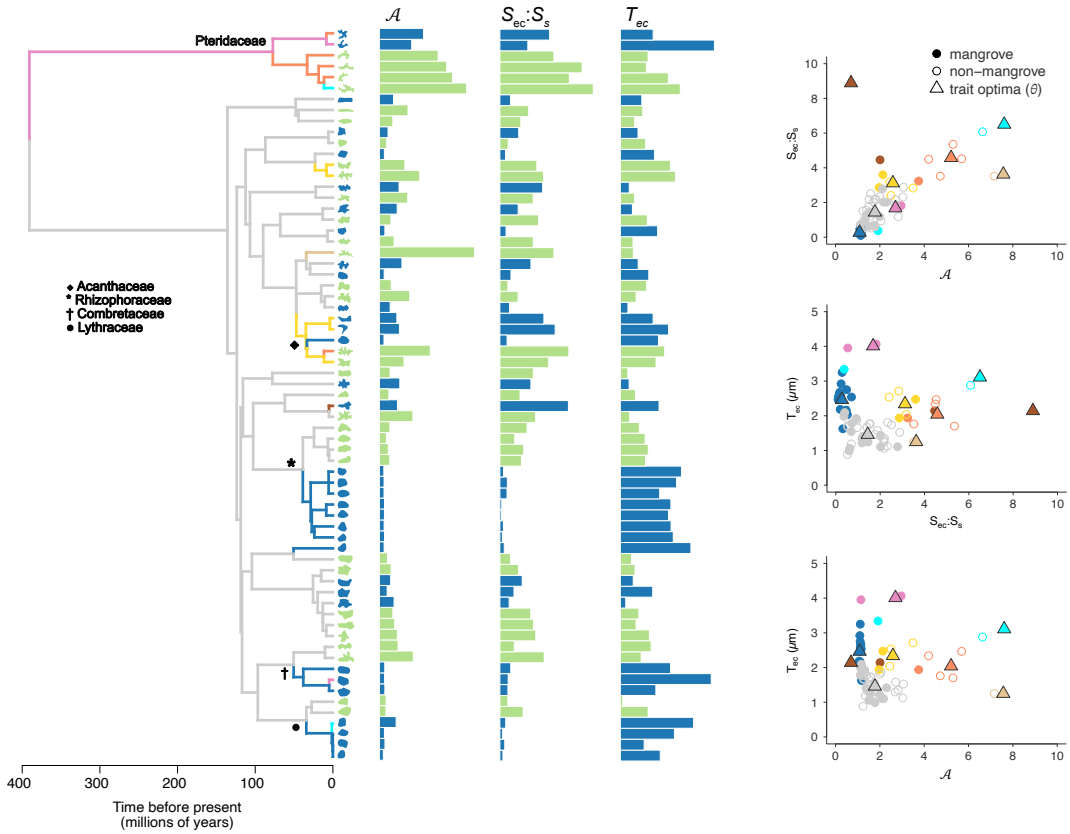

Figure 3. Mangrove lineages have experienced convergent evolution of leaf anatomy because of cell biomechanics. Mangroves and mangrove associates exhibit distinct traits and regimes of selection from their inland relatives. Branch colors on the phylogeny indicate selection regimes recovered by SURFACE analysis based on S_{ec}:S_s and T_{ec}. Images at the tips of the phylogeny are outlines of the median epidermal pavement cell per species. Bar charts show mean trait values for each species. For cell outlines and bar charts, green represents inland plant species and blue represents mangroves and mangrove associates. Scatterplots show the pairwise relationships among traits for mangroves (filled points) and non-mangroves (open points), as well as the modeled optimal trait values (triangles) returned by SURFACE. Points in scatterplots and branches on phylogeny are colored according to SURFACE regime. See also Figure S4.

STAR★METHODS

EXPERIMENTAL MODEL AND STUDY PARTICIPANT DETAILS

Mangrove and mangrove associate species were sampled from three natural reserves in southern China: Sanya Tielu Port Mangrove Natural Reserve (SY; 18°15′N/109°42′E), DongZhaiGang Mangrove Natural Reserve (DZG, 19°51′N/110°32′E), and ZhanJiang Mangrove Natural Reserve (ZJ, 20°14′N/109°40′E); while mangroves' inland relatives (non-mangroves) were sampled from three common gardens: Nanning Botanical Garden (NBG, 22°47′N/108°23′E), Xishuangbanna Tropical Botanical Garden (XTBG; 101°15'E/21°55'N), and the campus of Guangxi University (GXU, 22°50′N/108°17′E). All species for this study were listed as (Key Resources Table). At least 3-5 randomly selected individuals per species per site were selected for sampling. Sun-exposed branches were cut and sealed in a plastic bag with wet tissues, then transported back to the laboratory at Guangxi University for subsequent sample processing and measurements.

METHOD DETAILS

Anatomical measurements were processed according to our previous procedures [3]. All measurements were made on three to five randomly selected, fully expanded, healthy, sun-exposed leaves of each species. Three to five ~1-cm^2 sections of lamina were sampled from each leaf, avoiding the leaf margin and midrib. These sections were cleared in a 1: 1 solution of 30 % H2O2 and 100 % CH_3COOH and incubated at 70 °C until all pigments had been removed. The sections were then rinsed in water and the epidermises separated with forceps from the mesophyll and veins, allowing these three layers (upper epidermis, lower epidermis, and mesophyll with veins). Two layers of epidermis to be stained and mounted separately. To increase contrast, all samples were stained with Safranin O (1 % w/v in water) for 5~15 min and Alcian Blue (1 % w/v in 3 % acetic acid) for ~1 min, then washed in water and mounted on microscope slides. We also made cross-sections of the leaf lamina using a sliding microtome, and mounted these cross-sections on slides.

Images of sections on slides were taken at 20× or 40× magnification, which had fields of view of ~ 0.22 and 0.041 mm^2, respectively, using a compound microscope outfitted with a digital

camera (DM3000, Leica Inc., Germany) (Figure S1). Both abaxial (lower) and adaxial (upper) leaf surfaces were imaged for all species because some mangrove species were known to have stomata on both surfaces, as well as the leaf cross-sections for measurements on mesophyll cells. All anatomical measurements from images were made using ImageJ [39]. Epidermal pavement cell size (S_{ec}) and stomatal size (S_s) were quantified by measuring the two-dimensional areas of individual epidermal pavement cells and a guard cell pair (not including subsidiary cells), respectively (Figure S1). S_{ec} was measured on approximately 5 to 10 randomly chosen epidermal pavement cells that were not touching stomata in each image, while S_s was measured on approximately 5 guard cell pairs in each image. Perimeter of epidermal cells (P_{ec}) and the thicknesses of cell walls between two adjacent epidermal cells (T_{ec}) (Figure S1) were measured from light microscopy images from the same cells measured for S_{ec}, following the method of Vieira and Roddy [20]. Epidermal pavement cell shape acircularity ($\mathcal{A}$) was calculated following [40] as:

$$\mathcal{A} = \frac{{P_{ec}}^2}{4\pi S_{ec}},$$

which is dimensionless and scaled such that $\mathcal{A} = 1$ for a perfect circle and is higher than 1 for increasingly acircular shapes. From cross-sections of the leaf lamina, we measured the cell wall thickness between two adjacent cells of palisade and spongy mesophyll cells using the same method as used for T_{ec}. Stomatal density (D_s) was measured by counting the number of stomata (~20-30 cells/image) and dividing by the area of the field of view. We calculated the maximum stomatal conductance ($g_{s,max}$) from measurements of S_s and D_s following the method of Franks and Beerling [41], where guard cells were assumed to be shaped as idealized capsules [17] with length twice their width and the diameter of their hemispherical ends equal to the height of their central cylinder, such that guard cell length is equal to $4\sqrt{\frac{S_s}{2(\pi+4)}}$.

Genome size

The genome sizes of twelve mangrove species studied were taken from the literature [1]. Measurements of genome size in megabases (Mb) were converted to picograms (pg) following the equation 1 pg = 1 Mb / 978 [42]. Additionally, we measured genome sizes of

Senna surattensis, *Hibiscus rosa-sinensis* var. *rubro-plenus*, *Sterculia monosperma*, *Allamanda schottii*, *Handroanthus chrysanthus* from fresh leaves collected from GXU using flow cytometry (BD Accuri C6, Becton, Dickinson and Company, NJ, USA), using the procedure of [43]. Otto solution protocols from Dolezel et al. (2007) were followed, and leaves of *K. obovata* and *Oryza sativa* L. ssp. *indica* were used as reference genome sizes. The flow rate of the cytometer was set to 20 - 50 nuclei per second and 10,000 counts were collected. Plot counts were analyzed using FlowJo 7.6, and genome size was calculated as described previously [43].

QUANTIFICATION AND STATISTICAL ANALYSIS

All statistical analyses were conducted in R (v.4.5.1). For analyses that incorporated shared evolutionary history, a phylogeny was constructed using the R package V. Phylomaker2 [44]. To determine differences in trait values between mangroves and non-mangroves, we used phylogenetic analysis of variance (phylANOVA in package 'phytools') with log-transformed trait values. To determine the scaling relationships between traits, we used standard major axis regression, as implemented in the R package 'smatr', with an interaction term of habitat. Slope tests and elevation tests were implemented in 'smatr' [45].

To fit models of multivariate trait evolution, we used the R package 'mvMORPH'. First, we simulated stochastic character maps of habitat on the phylogenetic tree for 1000 histories of habitat occupation [33]. These 1000 trees were then used in subsequent models of trait evolution. We fit Brownian motion and Ornstein-Uhlenbeck (OU) models of multivariate trait evolution, using versions of these models that did (BMM, OUM) and did not (BM1, OU1) allow for each trait to have different optimal values for mangroves and non-mangroves. The best-fitting model was determined for each tree based on a difference in AIC of at least 2 (Figures S2 and S3). Second, to test for convergent evolution, we used the R package 'SURFACE' [34] to identify based solely on the phylogeny and traits (i.e. without *a priori* specification of habitat) which lineages have experienced similar regimes of selection. Both types of models were fit using the three traits (T_{ec}, S_{ec}:S_s, and $\mathcal{A}$) that exhibited the largest differences between mangroves and non-mangroves in earlier analyses, as well as using only

T_{ec} and S_{ec}:S_s, which showed larger differences than $\mathcal{A}$. Additionally, S_{ec}:S_s was chosen over incorporating S_{ec} and S_s separately because S_s controls for the background variation in cell size due to genome size variation and the specific hypothesis was about S_{ec} relative to S_s.

380 Evolutionary models were fit on scaled and centered trait data, and modeled optimal trait values (θ) generated by OU models were back-transformed for presentation.

REFERENCES

1. He, Z., Feng, X., Chen, Q., Li, L., Li, S., Han, K., Guo, Z., Wang, J., Liu, M., Shi, C., et al. (2022). Evolution of coastal forests based on a full set of mangrove genomes. Nat Ecol Evol *6*, 738–749. https://doi.org/10.1038/s41559-022-01744-9.
2. Tomlinson, P.B. (2016). The Botany of Mangroves, 2nd edition Edition (Cambridge University Press).
3. Jiang, G.F., Li, S.Y., Dinnage, R., Cao, K.F., Simonin, K.A., and Roddy, A.B. (2023). Diverse mangroves deviate from other angiosperms in their genome size, leaf cell size and cell packing density relationships. Annals of botany *131*, 347–360. https://doi.org/10.1093/aob/mcac151.
4. Jiang, G.F., Li, S.Y., Li, Y.C., and Roddy, A.B. (2022). Coordination of hydraulic thresholds across roots, stems, and leaves of two co-occurring mangrove species. Plant Physiology *189*, 2159–2174. https://doi.org/10.1093/plphys/kiac240.
5. Jiang, G.F., Brodribb, T.J., Roddy, A.B., Lei, J.Y., Si, H.T., Pahadi, P., Zhang, Y.J., and Cao, K.F. (2021). Contrasting Water Use, Stomatal Regulation, Embolism Resistance, and Drought Responses of Two Co-Occurring Mangroves. Water *13*. https://doi.org/ARTN 1945 10.3390/w13141945.
6. Jiang, G.F., Goodale, U.M., Liu, Y.Y., Hao, G.Y., and Cao, K.F. (2017). Salt management strategy defines the stem and leaf hydraulic characteristics of six mangrove tree species. Tree Physiology *37*, 389–401. https://doi.org/10.1093/treephys/tpw131.
7. Reef, R., and Lovelock, C.E. (2015). Regulation of water balance in mangroves. Annals of botany *115*, 385–395. https://doi.org/10.1093/aob/mcu174.
8. Ball, M.C. (1988). Ecophysiology of mangroves. Trees *2*, 129–142. https://doi.org/10.1007/BF00196018.
9. Theroux-Rancourt, G., Roddy, A.B., Earles, J.M., Gilbert, M.E., Zwieniecki, M.A., Boyce, C.K., Tholen, D., McElrone, A.J., Simonin, K.A., and Brodersen, C.R. (2021). Maximum CO2 diffusion inside leaves is limited by the scaling of cell size and genome size. Proc Biol Sci *288*, 20203145. https://doi.org/10.1098/rspb.2020.3145.
10. Simonin, K.A., and Roddy, A.B. (2018). Genome downsizing, physiological novelty, and the global dominance of flowering plants. Plos Biol *16*, e2003706. https://doi.org/10.1371/journal.pbio.2003706.
11. de Boer, H.J., Eppinga, M.B., Wassen, M.J., and Dekker, S.C. (2012). A critical transition in leaf evolution facilitated the Cretaceous angiosperm revolution. Nat Commun *3*, 1221. https://doi.org/10.1038/ncomms2217.
12. Carins Murphy, M.R., Jordan, G.J., and Brodribb, T.J. (2014). Acclimation to humidity modifies the link between leaf size and the density of veins and stomata. Plant, Cell & Environment *37*, 124–131. https://doi.org/10.1111/pce.12136.
13. Farquhar, G.D., and Sharkey, T.D. (1982). Stomatal Conductance and Photosynthesis. Annual Review of Plant Biology *33*, 317–345. https://doi.org/10.1146/annurev.pp.33.060182.001533.
14. Zuch, D.T., Doyle, S.M., Majda, M., Smith, R.S., Robert, S., and Torii, K.U. (2021). Cell biology of the leaf epidermis: Fate specification, morphogenesis, and coordination. The Plant cell *34*, 209–227. https://doi.org/10.1093/plcell/koab250.
15. Onoda, Y., Schieving, F., and Anten, N.P.R. (2015). A novel method of measuring leaf epidermis and mesophyll stiffness shows the ubiquitous nature of the sandwich structure of leaf laminas in broad-leaved angiosperm species. Journal of experimental botany *66*, 2487–2499. https://doi.org/10.1093/jxb/erv024.
16. Baresch, A., Crifò, C., and Boyce, C.K. (2019). Competition for epidermal space in the evolution of leaves with high physiological rates. New Phytologist *221*, 628–639. https://doi.org/10.1111/nph.15476.

17. Roddy, A., Theroux-Rancourt, G., Abbo, T., Brodersen, C.R., Jensen, B.M., Jiang, G.-F., Thompson, R.A., Kuebbing, S.E., and Simonin, K.A. (2020). The scaling of genome size and cell size limits maximum rates of photosynthesis with implications for ecological strategies. International Journal of Plant Sciences *181*, 75–87. https://doi.org/10.1086/706186.
18. Šímová, I., and Herben, T. (2012). Geometrical constraints in the scaling relationships between genome size, cell size and cell cycle length in herbaceous plants. Proceedings of the Royal Society B: Biological Sciences *279*, 867–875. https://doi.org/doi:10.1098/rspb.2011.1284.
19. Carins Murphy, M.R., Jordan, G.J., and Brodribb, T.J. (2012). Differential leaf expansion can enable hydraulic acclimation to sun and shade. Plant, Cell & Environment *35*, 1407–1418. https://doi.org/10.1111/j.1365-3040.2012.02498.x.
20. Goncalves, D.V., and Roddy, A.B. (2025). Leaf hydraulic traits change in coordination with cell size and cell shape throughout leaf development in a tropical fern. Annals of botany. 10.22541/au.174591010.01366146/v1.
21. Sapala, A., Runions, A., Routier-Kierzkowska, A.-L., Das Gupta, M., Hong, L., Hofhuis, H., Verger, S., Mosca, G., Li, C.-B., Hay, A., et al. (2018). Why plants make puzzle cells, and how their shape emerges. eLife *7*, e32794. https://doi.org/10.7554/eLife.32794.
22. Hamant, O., Heisler, M.G., Jönsson, H., Krupinski, P., Uyttewaal, M., Bokov, P., Corson, F., Sahlin, P., Boudaoud, A., Meyerowitz, E.M., et al. (2008). Developmental Patterning by Mechanical Signals in Arabidopsis. Science *322*, 1650–1655. https://doi.org/10.1126/science.1165594.
23. Zörb, C., Mühling, K.H., Kutschera, U., and Geilfus, C.-M. (2015). Salinity stiffens the epidermal cell walls of salt-stressed maize leaves: is the epidermis growth-restricting? PloS one *10*, e0118406–e0118406. https://doi.org/10.1371/journal.pone.0118406.
24. Kutschera, U., and Köhler, K. (1994). Cell elongation, turgor and osmotic pressure in developing sunflower hypocotyls. Journal of experimental botany *45*, 591–595. https://doi.org/10.1093/jxb/45.5.591.
25. Nieves-Cordones, M., Azeem, F., Long, Y., Boeglin, M., Duby, G., Mouline, K., Hosy, E., Vavasseur, A., Chérel, I., Simonneau, T., et al. (2022). Non-autonomous stomatal control by pavement cell turgor via the K+ channel subunit AtKC1. The Plant cell *34*, 2019–2037. https://doi.org/10.1093/plcell/koac038.
26. Franks, P.J., and Farquhar, G.D. (2007). The mechanical diversity of stomata and its significance in gas-exchange control. Plant Physiology *143*, 78–87. https://doi.org/10.1104/pp.106.089367.
27. Touchette, B.W., Marcus, S.E., and Adams, E.C. (2014). Bulk elastic moduli and solute potentials in leaves of freshwater, coastal and marine hydrophytes. Are marine plants more rigid? AoB Plants *6*. https://doi.org/10.1093/aobpla/plu014.
28. Vofely, R.V., Gallagher, J., Pisano, G.D., Bartlett, M., and Braybrook, S.A. (2019). Of puzzles and pavements: a quantitative exploration of leaf epidermal cell shape. New Phytologist *221*, 540–552. https://doi.org/10.1111/nph.15461.
29. Westgate, M.E., and Boyer, J.S. (1985). Osmotic adjustment and the inhibition of leaf, root, stem and silk growth at low water potentials in maize. Planta *164*, 540–549. https://doi.org/10.1007/BF00395973.
30. Handa, S., Bressan, R.A., Handa, A.K., Carpita, N.C., and Hasegawa, P.M. (1983). Solutes contributing to osmotic adjustment in cultured plant cells adapted to water stress. Plant Physiol *73*, 834–843. https://doi.org/10.1104/pp.73.3.834.
31. Silveira, S.R., Collet, L., Haque, S.M., Lapierre, L., Bagniewska-Zadworna, A., Smith, R.S., Gosselin, F.P., Routier-Kierzkowska, A.-L., and Kierzkowski, D. (2025). Mechanical interactions between tissue layers underlie plant morphogenesis. Nature Plants *11*, 909–923. https://doi.org/10.1038/s41477-025-01944-8.

32. Terashima, I., Miyazawa, S.I., and Hanba, Y.T. (2001). Why are sun leaves thicker than shade leaves? Consideration based on analyses of CO2 diffusion in the leaf. Journal of Plant Research *114*, 93–105. https://doi.org/10.1007/Pl00013972.

33. Huelsenbeck, J.P., Nielsen, R., and Bollback, J.P. (2003). Stochastic Mapping of Morphological Characters. Systematic Biology *52*, 131–158. https://doi.org/10.1080/10635150390192780.

34. Ingram, T., and Mahler, D.L. (2013). SURFACE: detecting convergent evolution from comparative data by fitting Ornstein-Uhlenbeck models with stepwise Akaike Information Criterion. Methods in Ecology and Evolution *4*, 416–425. https://doi.org/10.1111/2041-210X.12034.

35. Cosgrove, D.J. (2005). Growth of the plant cell wall. Nature Reviews Molecular Cell Biology *6*, 850–861. https://doi.org/10.1038/nrm1746.

36. Sugiura, D., Terashima, I., and Evans, J.R. (2020). A Decrease in Mesophyll Conductance by Cell-Wall Thickening Contributes to Photosynthetic Downregulation. Plant Physiology *183*, 1600–1611. 10.1104/pp.20.00328.

37. Gago, J., Carriquí, M., Nadal, M., Clemente-Moreno, M.J., Coopman, R.E., Fernie, A.R., and Flexas, J. (2019). Photosynthesis Optimized across Land Plant Phylogeny. Trends in plant science *24*, 947–958. https://doi.org/10.1016/j.tplants.2019.07.002.

38. Veromann-Jürgenson, L.L., Tosens, T., Laanisto, L., and Niinemets, Ü. (2017). Extremely thick cell walls and low mesophyll conductance: welcome to the world of ancient living! Journal of experimental botany *68*, 1639–1653. https://doi.org/10.1093/jxb/erx045.

39. Rueden, C.T., Schindelin, J., Hiner, M.C., DeZonia, B.E., Walter, A.E., Arena, E.T., and Eliceiri, K.W. (2017). ImageJ2: ImageJ for the next generation of scientific image data. Bmc Bioinformatics *18*, 529. https://doi.org/10.1186/s12859-017-1934-z.

40. Treado, J., Roddy, A., Theroux-Rancourt, G., Zhang, L., Ambrose, C., Brodersen, C., Shattuck, M., and O'Hern, C. (2022). Localized growth and remodelling drives spongy mesophyll morphogenesis. Journal of The Royal Society Interface *19*. https://doi.org/10.1098/rsif.2022.0602.

41. Franks, P.J., and Beerling, D.J. (2009). Maximum leaf conductance driven by CO2 effects on stomatal size and density over geologic time. Proceedings of the National Academy of Sciences *106*, 10343–10347. https://doi.org/10.1073/pnas.0904209106.

42. Dolezel, J., Bartoš, J., Voglmayr, H., and Greilhuber, J. (2003). Nuclean DNA content and Genome Size of Trout and Human. Cytometry. Part A : the journal of the International Society for Analytical Cytology *51*, 127–128; author reply 129. https://doi.org/10.1002/cyto.a.10013.

43. Dolezel, J., Greilhuber, J., and Suda, J. (2007). Estimation of nuclear DNA content in plants using flow cytometry. Nat Protoc *2*, 2233–2244. https://doi.org/10.1038/nprot.2007.310.

44. Jin, Y., and Qian, H. (2022). U.PhyloMaker: An R package that can generate large phylogenetic trees for plants and animals. Plant Diversity. https://doi.org/10.1016/j.pld.2022.12.007.

45. Warton, D.I., Duursma, R.A., Falster, D.S., and Taskinen, S. (2012). smatr 3 – an R package for estimation and inference about allometric lines. Methods in Ecology and Evolution *3*, 257–259. https://doi.org/10.1111/j.2041-210X.2011.00153.x.